Downloaded from rsta.royalsocietypublishing.org

PHILOSOPHICAL TRANSACTIONS OF THE ROYAL SOCIETY A MATHEMATICAL, PHYSICAL & ENGINEERING SCIENCES

Marangoni flows and corrosion of refractory walls

The Royal Society

Phil. Trans. R. Soc. Lond. A 1998 **356**, 1015-1026
doi: 10.1098/rsta.1998.0206

Email alerting service

Receive free email alerts when new articles cite this article - sign up in the box at the top right-hand corner of the article or click **here**

To subscribe to *Phil. Trans. R. Soc. Lond. A* go to: **http://rsta.royalsocietypublishing.org/subscriptions**

This journal is © 1998 The Royal Society

Downloaded from rsta.royalsocietypublishing.org

The Royal Society

Marangoni flows and corrosion of refractory walls

By Kusuhiro Mukai

Department of Materials Science and Engineering, Kyushu Institute of Technology, 1-1, Sensui-cho, Tobata-ku, Kitakyushu 804, Japan

Local corrosion of a refractory at slag–gas and slag–metal interfaces is caused by the active motion of slag film formed by the wettability between the refractory and slag. In the systems of SiO_2(s)–(PbO–SiO_2) slag and SiO_2(s)–Pb(l)–(PbO–SiO_2) slag, where components from the refractory dissolve into the slag increasing the interfacial tension of the slag or slag–metal, continuous washing of the refractory wall with thin fresh slag film supplied from the bulk slag phase by the Marangoni effect causes the local corrosion of the refractory above the slag level or below the metal level. When the dissolved component from the refractory reduces interfacial tension, for example, in the system of SiO_2(s)–(Fe_tO–SiO_2) slag, the local corrosion is induced by the active slag-film motion with alternative formation and disappearance in cyclic mode due to the Marangoni effect, and changes in the form of slag film due to the variation of interfacial tension and density of the slag film. Local corrosion of oxide refractories for practical use, containing trough materials, at slag–gas and slag–metal interfaces is classified into the above two types. The Maragoni flow of the slag film is also considered to play an important role in the local corrosion of oxide–graphite refractories such as Al_2O_3–C and MgO–C at the slag–metal interface during the stage of the oxide phase corrosion in the refractory.

Keywords: local corrosion; refractory; iron and steel making; slag surface; slag–metal interface; Marangoni flow

1. Introduction

It is well known that refractories composed of oxides, oxide–graphites and oxide–graphite–carbides are corroded locally at the slag–gas (slag surface) or slag–metal interface in glass technology and during iron and steel making processes. The local corrosion of refractories is a serious problem for these industries because it limits the life of the refractories. Several ideas had been proposed on the mechanism of the local corrosion. Jebsen-Marwedel (1956) proposed that the local corrosion of solid oxide by molten glass is caused by interfacial turbulence of the molten glass induced by the Marangoni effect in the vicinity of the interface. Vago & Smith (1965) explain that a reactive vapour phase from a liquid glass plays an important role in the local corrosion of solid oxide, with the form of a neck above glass level. Caley *et al.* (1981) state that oxygen gas in the atmosphere is the main cause for the local corrosion of solid oxide by molten PbO–SiO_2 slag. Brückner (1967), Sendt (1965) and Schulte (1977) have estimated that local corrosion of the solid oxide at the slag–metal interface is also caused by an interfacial turbulence of molten glass induced by the Marangoni effect in the vicinity of the interface. Iguchi *et al.* (1979)

© 1998 The Royal Society
TEX Paper

Downloaded from rsta.royalsocietypublishing.org

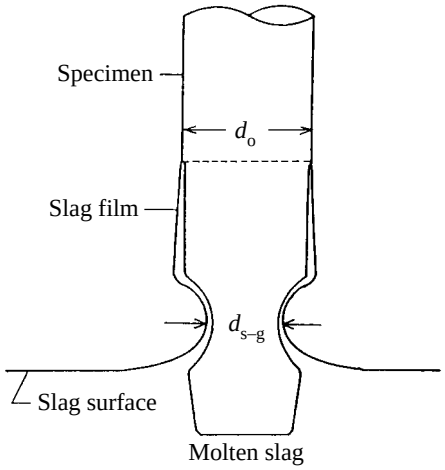

Figure 1. Typical local corrosion profile of the SiO_2(s)–(PbO–SiO_2) slag system (Mukai *et al.* 1983).

explained the local corrosion of solid alumina at the slag–metal interface based on the model of electrochemical reaction. Since 1983, authors have been investigating the local corrosion of refractories at the interfaces of slag–gas and slag–metal by combining optical or X-ray radiographic technique-aided direct observation of the phenomenon, which occurs in the local corrosion zone with a conventional immersion test in the following systems: (1) solid silica (SiO_2(s))–(PbO–SiO_2) slag; (2) SiO_2(s)–Pb(l)–(PbO–SiO_2) slag; (3) SiO_2(s)–(Fe_tO–SiO_2) slag; (4) SiO_2(s)–(Na_2O–SiO_2) slag; (5) magnesia-chrome refractory–(CaO–Al_2O_3–SiO_2) slag; (6) magnesia-chrome refractory–Fe(l)–(CaO-Al_2O_3–SiO_2) slag; (7) blast furnace trough material–(CaO–Al_2O_3–SiO_2) slag; (8) the trough material–Fe–C alloy(l)–(CaO–Al_2O_3–SiO_2) slag; (9) Al_2O_3–C refractory–Fe-C alloy(l)–(CaO–Al_2O_3–SiO_2) slag; and (10) MgO–C refractory–Fe(l)–(CaO–Al_2O_3–SiO_2) slag.

2. Local corrosion of SiO_2(s)–slag and SiO_2(s)–Pb(l)-slag systems

(*a*) SiO_2(s)–(PbO–SiO_2) *slag system (Mukai et al. 1983, 1984a, 1985, 1986a, b)*

Immediately after partially immersing the SiO_2 specimen in PbO–SiO_2 slag at 1073 K in an Ar atmosphere, slag begins to creep up the specimen surface to form slag film above the slag level. The active slag-film motion can be directly observed and recorded on cinefilm with the aid of the movement of very small bubbles in the slag film. The local corrosion of this system, as shown in figure 1, progresses in the area where the slag film moves actively. When platinum wire is tightly wound on the surface of the SiO_2 specimen at, and around, the slag level, the wire prevents the slag film moving and the local corrosion does not occur. Oxygen content in the atmosphere does not affect the local corrosion rate. The above experimental results indicate that neither a reactive vapour phase, nor oxygen in the atmosphere, is the main cause of the local corrosion of this system.

The slag film forms characteristic flow patterns, principally composed of wide zones of rising film and narrow zones of falling film, according to the contour of the specimen, as shown in figures 2 and 3. In the case of a cylindrical specimen, the position of the falling zone moves gradually on the surface of the specimen. However,

Downloaded from rsta.royalsocietypublishing.org

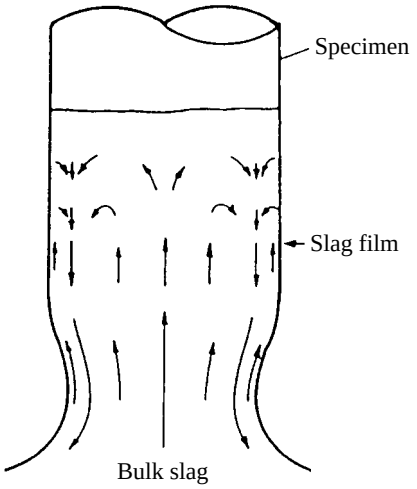

Figure 2. Typical flow pattern of the slag film on the 6 mm OD silica specimen dipped in $PbO–SiO_2$ slag (Mukai *et al.* 1985).

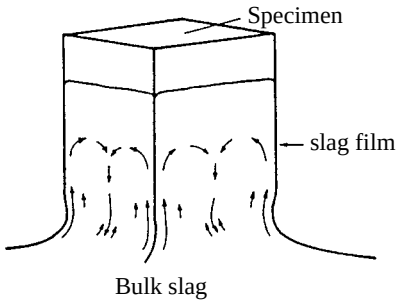

Figure 3. Typical flow pattern of the slag film of a 6 mm square prism specimen (Mukai *et al.* 1985).

the prism-shaped specimen always has one zone of rising film at, and around, each corner of the specimen and one narrow zone of falling film at each plane side of the specimen, as shown in figure 3.

Rising-zone films are several times thinner than falling-zone films. Change in SiO_2 content in rapidly solidified slag film is detected perpendicular to the specimen surface and also along the surface of the specimen in the vertical direction. Since contact time of the upper film with the specimen is longer than that for the lower film, the upper film has a higher SiO_2 content, due to the dissolution of SiO_2 from the specimen into the film. The difference in SiO_2 content causes a surface tension gradient in the vertical direction; for surface tension of $PbO–SiO_2$ slag increases with SiO_2 content (Hino *et al.* 1967). Thus the slag film is continuously pulled up by the surface tension gradient, i.e. the rising-zone of the film is generated by the Marangoni effect due to the concentration gradient. Since the film motion in the upper part of the specimen is slower than the lower part due to its high viscosity coefficient, the risen slag is accumulated in the upper part. The thickened film caused by the accumulation begins to fall down when its weight exceeds the surface tension gradient, i.e. a film falling zone is formed. Hydrodynamic analysis of the film motion, using the observed surface tension gradient along the surface of the film, results in good agreement between the calculated and observed film velocities. Velocity distribution

Downloaded from rsta.royalsocietypublishing.org

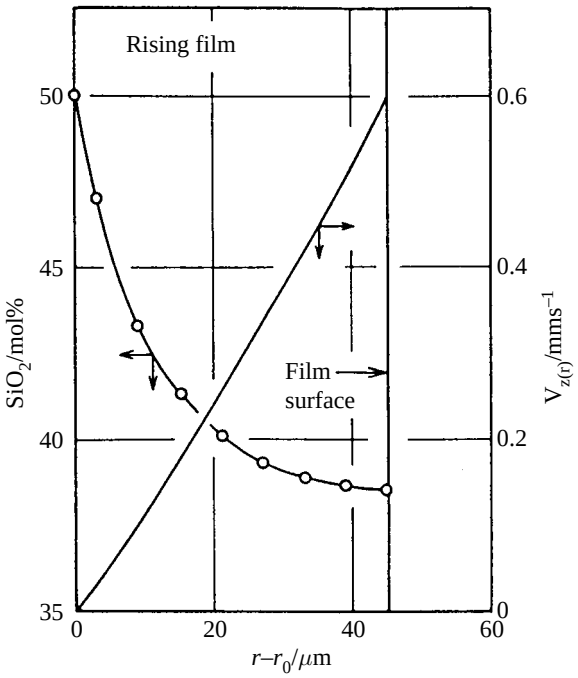

Figure 4. Distribution of velocity and SiO_2 content in the slag film for a 6 mm OD specimen dipped for 0.3 ks in a PbO–30 mol%SiO_2 slag at 1073 K (Mukai *et al.* 1985).

in the slag film obtained from the analysis shows that the slag film motion in the local corrosion zone is still active even in a thin slag film with a thickness of several tens of μm (figure 4). The film has a concentration gradient of SiO_2 perpendicular to the surface of the solid silica, which means that a diffusion layer is formed over the whole range of the slag film. The corrosion rate in the rising zone of the slag film is well-described by the rate equation derived from the conditions that the rate is controlled by mass transport of the dissolved component SiO_2 in the slag film under the Marangoni flow of the film. Therefore, the Marangoni flow in the slag film results in breakdown of the diffusion layer, which is the main cause of local corrosion. In other words, the local corrosion proceeds largely as a result of the wall-washing of solid silica with a fresh thin, rising slag film induced by the Marangoni effect. The corner of a prism specimen that is continuously washed always by the rising film, as shown in figure 3, is thus corroded much faster than the plane side, which leads to the formation of a round horizontal specimen cross section from an initial square-shaped cross section. On the other hand, a cylindrical specimen retains its initial round horizontal cross section in the local corrosion zone, because the rising zone of the slag film shifts its location with time on the surface of the specimen horizontally, resulting in an almost even corrosion rate at the same level in the local corrosion zone.

(*b*) *The* SiO_2(s)–(Fe_tO–SiO_2) *slag system (Yu & Mukai 1992; Yu 1995)*

Surface tension of PbO–SiO_2 slag is increased by the dissolved component SiO_2, as mentioned above, while SiO_2 reduces the surface tension of Fe_tO–SiO_2 slag (Yu 1995). Local corrosion and slag film motion in the local corrosion zone of this system can also be directly observed because the major part of the local corrosion zone

Downloaded from rsta.royalsocietypublishing.org

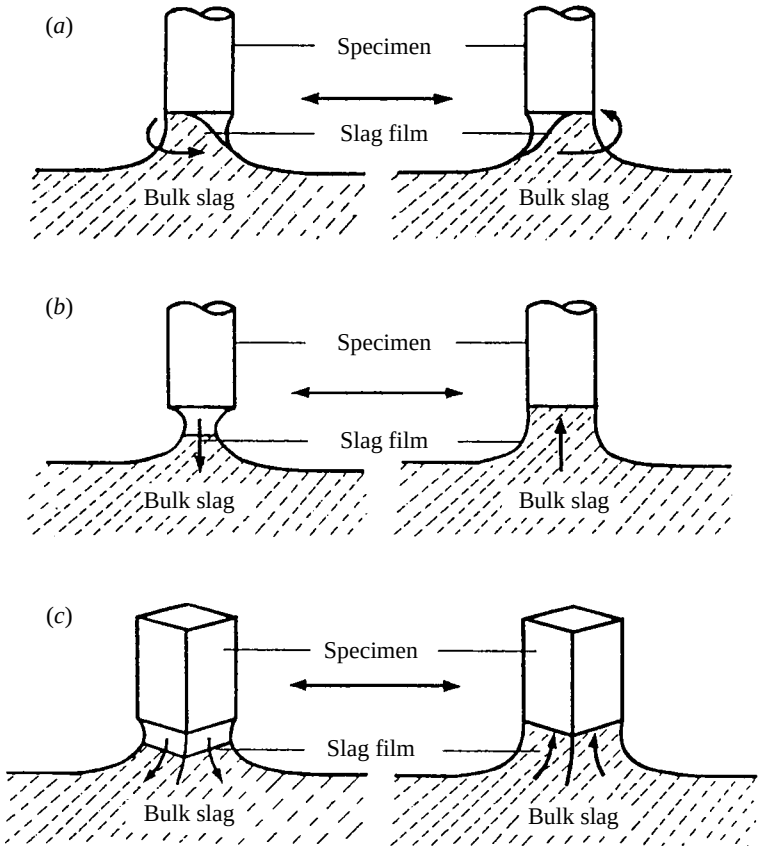

Figure 5. Slag film movements for rod and prism silica specimens dipped in a Fe_tO–SiO_2 slag (Yu & Mukai 1992): (*a*) rotational movement of slag film for the rod specimen; (*b*) up-and-down movement of slag film for the rod specimen; (*c*) up-and-down movement of slag film for the prism specimen.

occurs in the meniscus region of the slag (figure 5). The local corrosion zone of this system forms a steep groove and the vertical width of the local corrosion zone is narrower than that of the SiO_2(s)–(PbO–SiO_2) slag system. The slag film of this system has two types of characteristic motion. One is a rotational motion around the specimen surface during the initial stage of the local corrosion of the cylindrical specimen. The other is an up-and-down motion of the whole slag film along the specimen surface during the developed stage of the local corrosion of the cylindrical specimen, and during the entire stage of the corrosion of the prism specimen, as shown in figure 5. When the slag film motion is observed at a fixed point on the surface of the specimen, the film motion shows the following cyclic mode from stage 1 to 4: the slag film thickness (1) increases; (2) reaches a maximum state; (3) decreases; and (4) arrives at a minimum state, which is shown in figure 6. The slag film is formed during stage 1 within the local corrosion zone and disappears during stage 3. Figure 6 indicates that the maximum film thickness increases with increasing immersion time. The period of the cyclic motion increases linearly with increasing immersion time, which is qualitatively found from the increase in the space between adjacent lines in figure 6 with increasing immersion time. The shape of the slag film surface (meniscus shape) formed in the local corrosion zone is approximately described by a Laplace

Downloaded from rsta.royalsocietypublishing.org

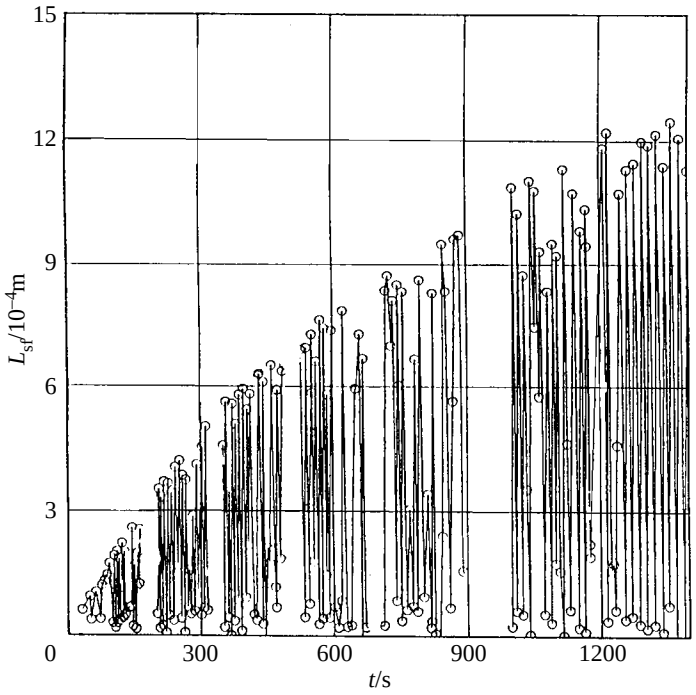

Figure 6. Change of slag film thickness in maximum local corrosion area, L_{sf}, with dipping time, t for a 75 mass%FeO–25 mass%SiO_2 slag with rod diameter 6 mm at 1623 K (Yu 1993).

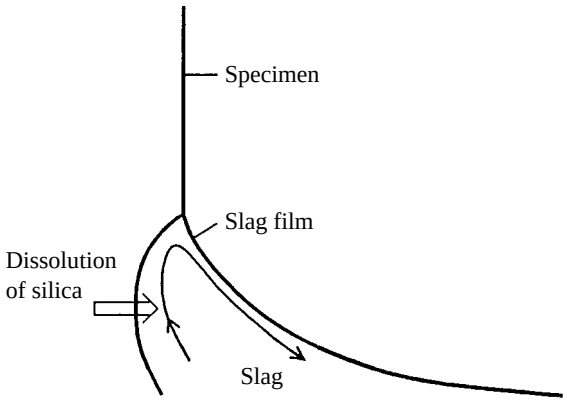

Figure 7. Marangoni convection of slag film in the local corrosion zone of a SiO_2(s)–(FetO–SiO_2) slag system.

equation, which includes σ/ρ, contact angle θ between slag and solid silica and rod diameter D as its main variables. σ and ρ are the surface tension and density of the slag, respectively. When θ is nearly constant, which is experimentally observed in this system, the slag film height (distance from slag level to the upper end of the slag meniscus) increases with increasing σ/ρ and D. The SiO_2 content in rapidly solidified slag film at stages 1 and 2 is lower than at stages 3 and 4, which means that σ/ρ is higher at stages 1 and 2 than at stages 3 and 4. Therefore, during stages 1 and 2, slag creeps up on the surface of the specimen and forms slag film and then reaches a maximum height. During stages 3 and 4 the slag film comes down and disappears.

Downloaded from rsta.royalsocietypublishing.org

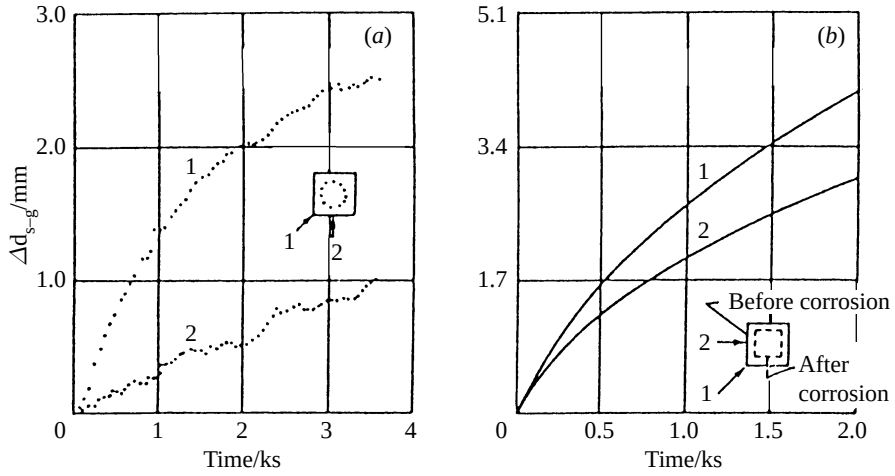

Figure 8. Comparison of the linear loss, Δd_{s-g}, at the planar part with that at the corner part of a prism specimen for: (*a*) SiO_2(s)–(PbO–SiO_2) slag, $T = 1073$ K (Mukai *et al.* 1983); (*b*) SiO_2(s)–(Fe_tO–SiO_2) slag $T = 1073$ K (Yu & Mukai 1992). $\Delta d_{s-g} = d_0 - d_{s-g}$ (see figure 1).

During stages 1–4, the SiO_2 content in the upper part of the slag film surface is higher than in the lower part of the surface. The SiO_2 content of the film decreases, reaches a minimum and then increases with distance from the slag film–specimen interface. The above change in SiO_2 content in the film indicates the continuous occurrence of the Marangoni flow in the film, as shown in figure 7, which accelerates the dissolution rate of the specimen into the slag film. The cyclic mode, with the formation and disappearance of the slag film, can be regarded as an analogous phenomenon to the surface renewal model proposed by Danckwerts (1951). The observed local corrosion rate of this system is reasonably explained by surface renewal theory. The corrosion rate at the corner of the prism specimen is $\sqrt{2}$ times as large as that at the plane. The cross-section of the prism specimen remains square during the entire corrosion process because the slag film has the same up-and-down motion at both the plane and corner sides, while in the SiO_2(s)–(PbO–SiO_2) slag system, the horizontal cross section of the prism specimen changes its shape from square to round, as shown in figure 8.

(*c*) *The* SiO_2(s)–(Na_2O) *slag system (Mukai & Yu 1993, unpublished work)*

SiO_2 scarcely decreases the surface tension of Na_2O–SiO_2 slag (King 1964). When the SiO_2 specimen is partially immersed in this slag, a slag film is also formed above the slag level. However, neither film motion nor the local corrosion is detected experimentally in this system.

(*d*) *The* SiO_2(s)–Pb(l)–(PbO–SiO_2) *slag system (Mukai et al. 1984b; 1989a)*

The Marangoni flow of the slag film in the local corrosion zone of the SiO_2(s)–Pb(l)–(PbO–SiO_2) slag system is induced by the concentration gradient of SiO_2 in the film at the interface between liquid lead and the slag film in the vertical direction (figure 9). The slag film motion was observed directly through the wall of a transparent silica crucible. Figure 9 shows that the flow pattern is composed primarily of a downward flow during the initial stage of the corrosion and then an upward film flow increases its frequency and area with time. The active Marangoni flow of the slag film with a thickness of several tens of μm accelerates the dissolution

Downloaded from rsta.royalsocietypublishing.org

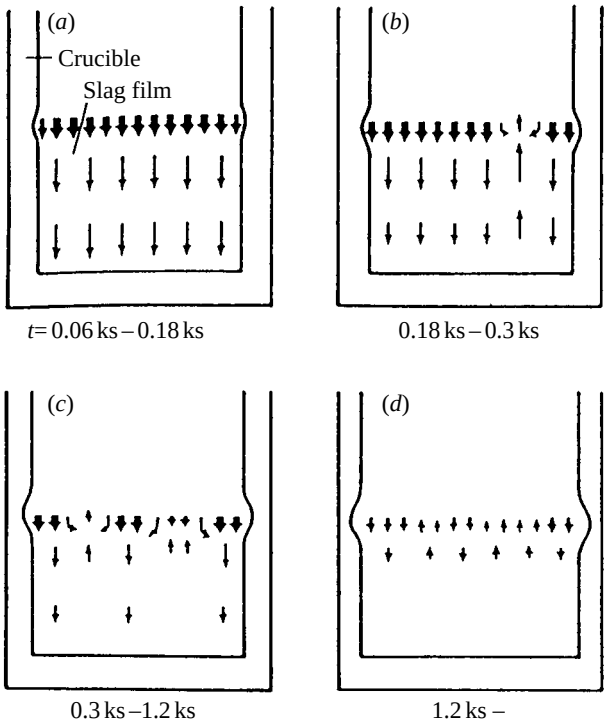

Figure 9. Schematic representation of the flow pattern of PbO–SiO_2 slag film formed between liquid lead and a silica crucible: t, elapsed time after the formation of the film (Mukai *et al.* 1989*a*).

rate of SiO_2 from the SiO_2 crucible into the film, resulting in local corrosion at the metal–slag interface. The manner in which local corrosion occurs in this system is essentially the same as that for the SiO_2(s)–(PbO–SiO_2) slag system when the phase of liquid lead is replaced with a gas phase and the present system is turned upside down.

3. Local corrosion of refractory for practical use: slag and the refractory–metal–slag systems

(*a*) *The magnesia–chrome refractory*–(CaO–Al_2O_3–SiO_2) *and the refractory*–Fe(l)–*slag system (Zainan et al. 1996; Mukai et al. 1995, unpublished work)*

The main corrosion modes of the magnesia–chrome refractory by the molten slag in the static condition are the local corrosion at interfaces of slag–gas and slag–metal, the pit-like corrosion at the bottom surface of the refractory specimen in the bulk slag phase and also in the upper part of the local corrosion zone. These corrosion modes were observed optically or by the aid of X-ray radiographic techniques.

The local corrosion rate at the slag surface increases with the iron oxide concentration of the slag and a decrease in the MgO and Al_2O_3 concentrations of the slag.

Both the local and pit-like corrosions are mainly caused by the Marangoni convection induced by the surface or interfacial tension difference along the interface

Downloaded from rsta.royalsocietypublishing.org

of the slag film which forms on the refractory specimen of the local corrosion zone, or the bubble surface near the bottom surface of the specimen. Direct observation confirmed that the flow pattern of the slag film along the rectangular specimen of the magnesia–chrome refractory in the local corrosion zone at the slag surface is similar to that shown in figure 3. Then, the interfacial tension difference is mainly caused by the concentration difference of MgO in the slag due to the dissolution of MgO from the refractory specimen into the slag.

(*b*) *The blast furnace trough material*–(CaO–Al_2O_3–SiO_2) *slag system (Mukai et al. 1984c, 1993)*

SiC granules on the surface of the trough material are oxidized by oxygen supplied from atmospheric gas via the slag film formed on the specimen of the material above the slag level, and are changed into carbon granules and SiO_2.

The dissolved SiO_2 from the trough material decreases the surface tension of CaO–Al_2O_3–SiO_2 slag (Mukai & Ishikawa 1981), which induces the slag film motion due to the Marangoni effect and the change in σ/ρ of the slag film. Slag film motion of this system is shown in figure 7. The flow mode of the meniscus was clarified by direct observation. Suspension of the carbon granules into the film and the slag film motion will facilitate the dissolution and abrasion of the trough material. Then, the local corrosion of this system arises only in an oxidizing atmosphere in the narrow zone of the trough material just above the slag level, though the slag film is also formed in an Ar atmosphere. Depth of the local corrosion increases in a step-like manner with time. This mode is analogous to that of the MgO(s)–(CaO–Al_2O_3–SiO_2) slag system (Harada *et al.* 1984). The limiting step of the corrosion rate for the rate retardation period is also considered to be the transport process of the accumulated SiO_2 from the slag surface into the bulk slag.

(*c*) *The blast furnace trough material*–Fe–C *alloy(l)*–(CaO-Al_2O_3–SiO_2) *slag system (Mukai et al. 1984d; Yoshitomi et al. 1986, 1987)*

The Marangoni flow of the slag film in the local corrosion zone of a metal–slag–trough material system is also induced by the concentration gradient of the slag film at the interface between the film and the metal in the vertical direction. The concentration gradient is caused by several kinds of reaction between the slag film and metal, or the film and the trough material, as shown in figure 10. The reaction (3.1) partially participates in the promotion of local corrosion by agitating the slag film as CO bubbles evolve:

$$(SiO_2) + 2\underline{C} \rightarrow \underline{Si} + CO(g). \tag{3.1}$$

Carbon particles generated by reaction (3.2) are suspended in the slag film and dissolve into the metal phase when the carbon concentration in the metal is low, thus accelerating local corrosion:

$$SiC(s) + 2(FeO) \rightarrow (SiO_2) + 2Fe(l) + C(s). \tag{3.2}$$

For metals containing high carbon content (e.g., in the vicinity of carbon saturation), suspended carbon particles remain in the slag film, which prevents motion of the film and reduces the contact area between the film and the metal, resulting in the reduction of the local corrosion rate.

Downloaded from rsta.royalsocietypublishing.org

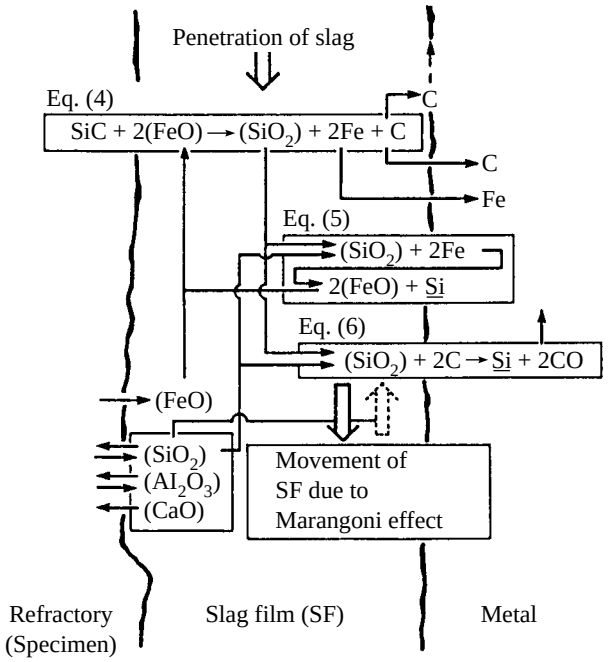

Figure 10. Transfer paths of reactant and products during the progress of local corrosion of trough materials at the slag–metal interface (Yoshitomi *et al.* 1987).

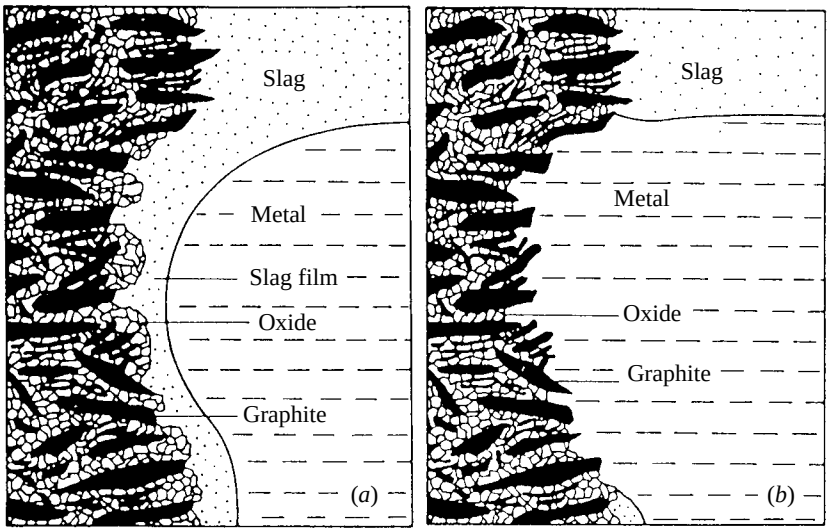

Figure 11. Schematic representation of the manner in which local corrosion of the immersion nozzle at the slag–metal interface proceeds (Mukai *et al.* 1989*b*).

(*d*) Al_2O_3–C *(Mukai et al. 1986b, 1989b) or* MgO–C *(Kii et al. 1995) refractories*–Fe(l)–(CaO-Al_2O_3–SiO_2) *slag system*

As shown in figure 11, when the wall of the Al_2O_3–C or MgO–C refractory is initially covered with a slag film (figure 11*a*), the film not only wets the oxides, but dissolves them in preference to graphite. This changes the interface to a graphite-rich layer. Since the metal phase wets graphite better than the slag, the metal phase creeps

Downloaded from rsta.royalsocietypublishing.org

up the surface of the specimen, as indicated in figure 11*b*, and dissolves graphite in preference to the oxides. Once the graphite-rich layer disappears due to dissolution into metal, the slag can again penetrate the boundary between the metal and the specimen, and the process is repeated. This cycle produces a local corrosion zone at the metal–slag interface. The up-and-down motion of the slag–metal interface shown in figure 11 was clearly observed using X-ray radiographic techniques.

The Marangoni flow of the slag film is also considered to play an important role in the local corrosion of immersion nozzles at the metal–slag interface during the stage shown in figure 11*a*.

4. Concluding remarks

Local corrosion of refractories at the slag surface is essentially caused by the active motion of the slag film formed by the wettability between the refractory and slag, since the slag film motion accelerates the dissolution rate of the refractory and also induces the abrasion of some refractories. The active film motion is dominantly induced by the Marangoni effect and/or change in the form of the slag film (slag meniscus) due to the variation of the surface tension and the density of the slag film.

The local corrosion of refractories at the slag–metal interface is also explained reasonably by a mechanism which is similar to that of the refractory–slag system. Then, the action of the surface (or interfacial) tension which leads to the local corrosion is very bad.

It is understood from this paper that the slag film of the SiO_2(s)–(PbO–SiO_2) slag system moves with a mechanism similar to the 'tears of strong wine' mechanism clarified by Thomson (1855) more than 130 years ago. The trivial phenomenon of 'wine's tear' holds the key to the solution of the industrially serious technological problem of the local corrosion of refractories.

References

Brückner, R. 1967 *Glastech. Ber.* **40**, 451.

Caley, W. F., Marple, B. R. & Masson, C. R. 1981 *Can. Metall. Q.* **20**, 215.

Danckwerts, P. V. 1951 *Ind. Eng. Chem.* **43**, 1460.

Harada, T., Fujimoto, S., Iwata, A. & Mukai, K. 1984 *J. Jap. Inst. Metals* **48**, 181.

Hino, M., Ejima, T. & Kameda, M. 1967 *J. Jap. Inst. Metals* **31**, 113.

Iguchi, Y., Yurek, G. J. & Elliott, J. F. 1979 *Proc. 3rd Int. Iron and Steel Cong. ASM*, p. 346.

Jebsen-Marwedel, H. 1956 *Glastech. Ber.* **29**, 233.

Kii, T., Hiragushi, K., Yasui, H. & Mukai, K. 1995 *Unified Int. Technical Conf. on Refractory, 4th Biennial Worldwide Conf. on Refractories, Japan*, p. 379.

King, T. B. 1964 *Trans. Met. Soc. AIME* **230**, 1671.

Mukai, K. & Ishikawa, T. 1981 *J. Jap. Inst. Metals* **45**, 147.

Mukai, K., Iwata, A., Harada, T., Yoshitomi, J. & Fujimoto, S. 1983 *J. Jap. Inst. Metals* **47**, 397.

Mukai, K., Nakano, T., Harada, T., Yoshitomi, J. & Fujimoto, S. 1984*a* *Proc. 2nd Int. Symp. on Metallurgical Slags and Fluxes*, p. 207. Pennsylvania, Met. Soc. AIME.

Mukai, K., Masuda, T., Gouda, K., Harada, T., Yoshitomi, J. & Fujimoto, S. 1984*b* *J. Jap. Inst. Metals* **48**, 726.

Mukai, K., Masuda, T., Yoshitomi, J., Harada, T. & Fujimoto, S. 1984*c* *Tetsu-to-Hagane* **70**, 823.

Downloaded from rsta.royalsocietypublishing.org

Mukai, K., Yoshitomi, J., Harada, T., Hurumi, K. & Fujimoto, S. 1984*d* *Tetsu-to-Hagane* **70**, 541.

Mukai, K., Harada, T., Nakano, T. & Hiragushi, K. 1985 *J. Jap. Inst. Metals* **49**, 1073.

Mukai, K., Harada, T., Nakano, T. & Hiragushi, K. 1986*a* *J. Jap. Inst. Metals* **50**, 63.

Mukai, K., Toguri, J. M. & Yoshitomi, J. 1986*b* *Can. Metall. Q.* **25**, 265.

Mukai, K., Gouda, K., Yoshitomi, J. & Hiragushi, K. 1989*a* *Proc. 3rd Int. Conf. on Molten Slags and Fluxes*, p. 215. London: The Institute of Metals.

Mukai, K., Toguri, J. M., Stubina, N. M. & Yoshitomi, J. 1989*b* *ISIJ Int.* **29**, 469.

Mukai, K., Ikeda, E. & Yu, Z. 1993 *1st Int. Conf. on Processing Materials for Properties, Hawaii*, p. 273.

Schulte, K. 1977 *Glastech. Ber.* **50**, 181.

Sendt, A. 1965 *7th Cong. Int. du Verre, Bruxelles*, 352.1.

Thomson, J. 1855 *Phil. Mag.* **10**, 330.

Vago, E. & Smith, C. E. 1965 *Proc. 7th Int. Congress Glass, Brussels*, vol. II, .1.2, 62.1-22.

Yoshitomi, J., Harada, T., Hiragushi, K. & Mukai, K. 1986 *Tetsu-to-Hagane* **72**, 411.

Yoshitomi, J., Hiragushi, K. & Mukai, K. 1987 *Tetsu-to-Hagane* **73**, 1535.

Yu, Z. 1993 Ph.D. thesis, Kyushu Institute of Technology, pp. 15–74, 145.

Yu, Z. & Mukai, K. 1992 *J. Jap. Inst. Metals* **56**, 1137.

Yu, Z. & Mukai, K. 1995 *J. Jap. Inst. Metals* **59**, 806.

Zainan, T., Mukai, K. & Ogata, M. 1996 *Taikabutsu* **48**, 568.